Human Molecular Genetics, 2000, Vol. 9, No. 9 **1259–1271**

ARTICLE

Decreased expression of striatal signaling genes in a mouse model of Huntington's disease

Ruth Luthi-Carter, Andrew Strand[1], Nikki L. Peters, Steven M. Solano, Zane R. Hollingsworth, Anil S. Menon, Ariel S. Frey, Boris S. Spektor, Ellen B. Penney, Gabriele Schilling[2], Christopher A. Ross[2], David R. Borchelt[2], Stephen J. Tapscott[1], Anne B. Young, Jang-Ho J. Cha and James M. Olson[1,+]

Department of Neurology, Massachusetts General Hospital, Boston, MA 02114, USA, [1]Human Biology Division, Fred Hutchinson Cancer Research Center, Seattle, WA 98109, USA, [2]Department of Neuropathology and [3]Department of Psychiatry, Johns Hopkins University School of Medicine, Baltimore, MD 21205, USA

Received 31 January 2000; Revised and Accepted 11 March 2000

To understand gene expression changes mediated by a polyglutamine repeat expansion in the human huntingtin protein, we used oligonucleotide DNA arrays to profile ~6000 striatal mRNAs in the R6/2 mouse, a transgenic Huntington's disease (HD) model. We found diminished levels of mRNAs encoding components of the neurotransmitter, calcium and retinoid signaling pathways at both early and late symptomatic time points (6 and 12 weeks of age). We observed similar changes in gene expression in another HD mouse model (N171-82Q). These results demonstrate that mutant huntingtin directly or indirectly reduces the expression of a distinct set of genes involved in signaling pathways known to be critical to striatal neuron function.

INTRODUCTION

Huntington's disease (HD) is an autosomal dominant neurodegenerative disorder manifested by psychiatric, cognitive and motor symptoms typically starting in mid life and progressing relentlessly to death. HD is caused by an expansion of a polyglutamine-encoding region in exon 1 of the *IT15* gene that encodes huntingtin (1). Although huntingtin is ubiquitously expressed, the medium spiny GABAergic cells of the striatum are preferentially damaged in HD. There is no cure for this disorder and there is currently no therapeutic approach to delay the onset of symptoms.

Positron emission tomography (PET) studies of presymptomatic human patients indicate that neurotransmitter receptor decreases occur prior to the onset of overt clinical symptoms (2). We have recently demonstrated decreases in neurotransmitter receptors in a transgenic mouse HD model which are selective in that certain receptors are decreased while others are not (3,4). The pattern of neurotransmitter receptor decreases cannot be attributed to degeneration of a specific population of cells, but rather appears to reflect down-regulation of a specific subset of genes. These receptor changes, which occur at the levels of both protein and mRNA, precede and may therefore contribute to the onset of clinical symptoms. A transcription-related mechanism of huntingtin toxicity can also be inferred from other recent studies (5–7). We therefore hypothesized that huntingtin-induced changes in gene expression might extend to functional categories besides neurotransmitter receptors and that understanding these changes might provide an insight into HD progression.

In the present study, we extended our previous analysis of gene expression in HD models to determine the scope of mRNAs affected by mutant huntingtin. Of nearly 6000 mRNAs that were measured, a small number were decreased, and these were remarkably restricted to genes encoding neurotransmitter, calcium and retinoid signaling pathway components. This study demonstrates that the decrease in the abundance of specific neurotransmitter receptors is associated with decreased expression of many genes that mediate the signaling response from these receptors. The data provide additional evidence that mutant huntingtin compromises the ability of striatal neurons to receive and integrate afferent input and establishes bases for rational therapeutic intervention.

RESULTS

We analyzed gene expression in the striata of R6/2 mice at both 6 and 12 weeks of age, representing stages of minimal and pronounced deterioration in neurological function, respectively (mice described in Materials and Methods). At each age, we extracted RNA from pooled striata of mice carrying the expanded exon 1 HD transgene and from wild-type littermate controls. Each RNA sample was divided in half and analyzed using two sets of Affymetrix murine expression arrays. Within

[+]To whom correspondence should be addressed. Tel: +1 206 667 7955; Fax: +1 206 667 6524; Email: jimmyo@u.washington.edu

each age group we made four comparisons: each data set from the HD transgenics to each of the two control data sets. Using the Affymetrix algorithm for assessing gene expression differences (8), we identified mRNAs that were increased or decreased in R6/2 mice relative to controls in all four comparisons (high stringency analysis). mRNAs that met this criterion are presented in Table 1A. We also analyzed the data by the criterion of three of four comparisons (moderate stringency analysis, Table 1B). Because confirmation studies in our laboratory demonstrated that the Affymetrix algorithm-based change calls are reliable even when the fold change is relatively small, no arbitrary thresholds were imposed on the data set (see Confirmation of microarray findings below, Criteria for selecting affected genes in Materials and Methods and www.neumetrix.com). Raw data and complementary data analyses (e.g. low stringency analysis and cross time point comparisons) are available at www.neumetrix.com . Using the three of four comparison cut-off, 1.7 and 1.2% of the genes tiled on the microarrays were changed in R6/2 mice compared with controls at 6 and 12 weeks, respectively. mRNAs that were decreased in R6/2 mice outnumbered those increased by 3:1. Increases were restricted largely to mRNAs associated with inflammatory and cell cycle function, while decreases were observed primarily in mRNAs involved in signal transduction, ion channels, transcription, metabolism and cell structure (Table 1 and Fig. 1). The representations of functional groups of molecules and the ratios between increased and decreased mRNAs obtained were similar using high, medium or low stringency criteria (Table 1 and www.neumetrix.com).

It is important to note that the striatum represents a mixed population of neurons and glia and, therefore, the reported fold change might not accurately reflect the magnitude of change within an affected sub-population of cells. It is likely, however, that most of the neuron-specific gene changes are attributable to GABAergic medium spiny neurons, since these represent >85% of the neuronal population in striatum. The microarray-based results are presented in the next sections and are followed by northern blot and *in situ* hybridization histochemistry (ISHH) analyses that confirm and extend the data from the expression arrays.

Reduced expression of genes central to neural signaling

The most striking finding of this study was the relatively restricted decrease in mRNAs that encode neuronal signaling molecules (Table 1). This study extends our previous observations that dopamine, glutamate and adenosine receptors are decreased in the R6/2 model of HD by demonstrating that multiple components of each of these signaling pathways are decreased at the mRNA level.

Neurotransmitter receptors, neurotransmitters and neuropeptides. Messenger RNAs encoding the G-protein-coupled receptors dopamine D_2, dopamine D_4, cannabinoid CB_1, adrenergic α_2 and an orphan glucocorticoid-inducible receptor (GIR) were decreased in R6/2 mice. Expression of the suspected HD modifier gene GluR6 (29) was also decreased. mRNAs for some receptor interacting proteins were affected, including α-actinin 2 (which was decreased) and the heterotrimeric G-protein subunit $G\gamma_3$ (which was increased). Decreases in mRNAs encoding the GABA-synthesizing enzyme glutamic acid decarboxylase and the neuropeptide precursors for enkephalin and somatostatin were also observed.

Signal transducing enzymes. Dysregulation of genes encoding signal transduction proteins in R6/2 mice extended beyond plasma membrane-bound receptors and involved many intracellular signaling components. These include adenylyl cyclases and phosphodiesterases, protein kinases and phosphatases, small G-proteins and inhibitors or regulatory subunits of these enzymes. These changes could affect synaptic transmission and plasticity, because the proteins in this category integrate, amplify and limit signals controlling many neuronal functions. In several instances, genes that encode proteins of opposing function are decreased. These balanced disruptions are consistent with the notion that expression of genes having opposing roles in signaling cascades is coordinately regulated. Even so, decreased expression of immediate early genes that are normally up-regulated by neuronal stimulation (Table 1) and reduced levels of adenylyl cyclase (see below) suggest that neuronal signal transduction is generally diminished.

Calcium homeostasis and mobilization. Calcium dysregulation has been postulated to be a component of HD pathology (30,31), but the mechanisms by which such changes occur have not been well defined. The present study revealed that this problem might be attributable, at least in part, to the down-regulation of mRNAs whose products regulate calcium homeostasis and calcium signaling. Calcium-related mRNAs that showed decreased expression in the R6/2 striata include a plasma membrane calcium ATPase (PMCA1AB), the type 1 ryanodine receptor (RYR1), the type 1 inositol 1,4,5-trisphosphate receptor (IP_3R1, P400), calcineurin, hippocalcin, a calmodulin-dependent phosphodiesterase (PDE1B1) and a calcium/calmodulin-dependent protein kinase (CAMK IV/Gr). In addition, many of the proteins in the signal transduction group are regulated or modulated by calcium and calcium-sensing proteins. One possible mechanism by which mutant huntingtin may cause calcium signaling disturbances is through physical association with a calmodulin-containing complex (32).

Nuclear hormone receptors. Retinoids (vitamin A derivatives) bind to nuclear hormone receptors and induce transcription of genes involved in neural differentiation and other processes (9). Expression of the striatally enriched retinoic acid receptor, RXRγ, and a retinol-binding protein was decreased in R6/2 striata compared with controls. In addition, >20% of the genes less abundantly expressed in R6/2 striatum contain retinoic acid response elements and are induced by retinoic acid receptor agonists in cell culture experiments (Tables 1A and 1B).

Unchanged expression of genes associated with neurodegenerative events or diabetes

Previous histopathological studies of R6/2 mice demonstrated that the striata of these animals show neither gross neuronal loss nor gliosis up to 13 weeks of age (33). Consistent with these findings, no decreases in the expression of axonal or dendritic neuronal marker genes (e.g. MAP2 or neurofilaments) or increases in the expression of glial marker genes

Table 1A. Differentially detected mRNAs (high stringency)

Call* 6 w 12 w	Fold Change* 6 w	12 w	Gene	Genbank #	Notes
			Signal Transduction		
	-3.7	-3.0	HIPPOCALCIN	P32078	S
	-1.8	-2.2	preproenkephalin	M13227	R, A
	-2.3	-2.6	protein phosphatase inhibitor 1	AA116737	E
	-1.8	-4.2	G-protein coupled receptor (GIR)	M80481	
	-5.1	-2.2	Ca/calmodulin dependent PK GR	P13234	E
	-2.3	-3.5	embryonic stem cell phosphatase (Esp)	U36488	
	-1.8	-3.9	calmodulin-dependent phosphodiesterase (PDE1B1)	L01695	R
	-5.1	-6.8	adenylyl cyclase, type V	W79953	R,E
	-2.1	1.0	adenylate cyclase, type II	Q08462	R,S
	-2.2	1.5	RHO-related GTP-binding protein RHOG	AA063858	E
	-2.2	-1.1	calcineurin B subunit	W47892	R,E
	-3.1	-1.6	calcineurin B subunit isoform 1	P06705	R,S
	-4.1	1.3	D4 dopamine receptor	U19880	R
	-2.3	-1.1	c-mer tyrosine kinase receptor	U21301	
	-1.9	-1.3	protein kinase C-gamma	L28035	
	-9.8	-1.7	serine/threonine protein kinase SGK	Q09226	S
	-2.6	1.3	inhibitor protein of cAMP-dependent protein kinase	M63554	
	-1.3	-1.9	protein kinase C beta-II	X53532	
	1.2	-3.5	GluR6 (glutamate receptor beta-2 subunit)	X66117	R
	-1.2	-2.0	protein tyrosine phosphatase STEP61	U28217	
	-1.1	-2.4	RAP1 GTPase activating protein (RAP1GAP)	AA013851	E
	1.3	-2.2	RAP1 GTPase activating protein (RAP1GAP)	W11780	E
	1.1	2.4	G-protein G(i)/G(S)/G(O) gamma-3 subunit	AA049022	E
			Ion Channels		
	-1.9	-2.3	calcium-transporting ATPase (PMCA1AB)	W97373	A,E
	-2.2	-2.4	cerebellum P400 protein (IP3 receptor)	X15373	
	-3.9	-4.9	RyR1 ryanodine receptor	X83932	R
	-3.9	-3.4	inwardly-rectifying K+ channel protein (mb-IRK3)	U11075	
	-1.7	-1.8	potassium channel beta-1 subunit	X97281	
	-1.1	-1.6	voltage-dependent sodium channel beta-1 subunit	L48667	
			Transcription		
	-2.8	-2.9	zif268 (NGFI-A)	M22326	R, A
	-1.4	-3.0	N10 (NGFI-B) (NUR77)	X16995	A
	-5.0	-1.5	Meis2	U57343	R
	-1.8	-1.5	retinol binding protein (RBP)	W14367	R,E
	-1.2	-3.1	junB	J03236	R, A
	-1.4	-3.9	albumin gene D-Box binding protein	U29762	
			Stress or Inflammatory Response		
	1.8	1.6	immunophilin P59	X70867	
	1.2	2.7	MHC class I B(2)-microglobulin (W4 allele)	AA059700	I,E
			Cell Cycle		
	2.4	1.5	topoisomerase I	D10061	I
	1.1	1.7	PCNA (DNA polymerase delta auxiliary protein)	X57800	
	1.8	3.0	Xeroderma Pigmentosum group A correcting gene	X74351	
	1.8	2.7	caltractin (centrin)	AA153569	E
	1.5	2.0	gas5 (growth arrest specific protein)	X59728	I
			Cytoskeleton and Cell Adhesion		
	-1.6	-1.9	telencephalin (ICAM-5)	U06483	
	-1.2	-2.1	alpha-actinin 2 (F-actin cross linking protein)	W34429	E
	-1.6	-1.8	gas 3 (Peripheral Myelin Protein 22)	M32240	
	2.0	1.5	alpha-tubulin isotype M-alpha-2	M13445	
	3.1	3.4	tctex-1	W15873	E
	1.3	2.4	troponin C	W29418	E
			Metabolism		
	-2.7	-5.8	phosphatidylcholine transfer protein (PCTP)	W41070	E
	-3.2	1.1	gamma (neuron specific) enolase	P07323	R, A, S
	-1.8	-1.2	fatty acid transport protein (FATP)	U15976	
	-1.7	-1.8	endoplasmic reticulum protein ERP99/GRP94	M77003	
	-1.9	-1.1	creatine kinase B chain	P07335	S
	-1.5	-1.4	creatine kinase B	M74149	A
	-1.8	-2.0	indoleamine 2,3-dioxygenase	M69109	
	3.9	1.5	brain fatty acid-binding protein (B-FABP)	U04827	
	2.5	-1.2	hydroxysteroid sulfotransferase (mSTa2)	L27121	
			Miscellaneous		
	-3.3	-3.7	brain protein H5 (septin CDCrel-1)	AA020101	E
	-2.3	-2.2	alpha2,8-sialyltransferase	X80502	
	-4.3	1.0	similar to signal sequence receptor gamma subunit	W78418	E
	-2.5	-1.2	cytoplasmic protein Ndr1	U60593	
	-2.7	-1.2	21K protein	W46015	E
	-3.2	-1.3	pantophysin	AA057362	E
	-1.8	1.2	probable phosphoserine aminotransferase (EPIP)	AA068780	E
	-1.8	-1.3	similar to IER5	AA013648	E
	-1.5	-1.2	zinc finger protein (MOK2)	M32057	
	-1.7	-2.1	clathrin-associated protein 19 (AP19)	M62418	
	2.6	1.3	DNA-binding protein	L20450	
	4.9	-1.3	MP4 gene for a proline-rich protein	X58438	
	1.7	1.4	Int-6 / eIF3 P48	L35556	

Table 1B. Differentially detected mRNAs (moderate stringency)

Call* 6 w 12 w	Fold Change* 6 w	12 w	Gene	Genbank #	Notes
			Signal Transduction		
	-1.6	-2.6	D2A dopamine receptor	X55674	R
	-2.3	1.4	probable G-protein coupled receptor EDG-1	P48303	S
	-1.6	-1.5	serine/threonine protein kinase SGK	AA163305	E
	-1.4	1.2	mouse developmental kinase 2 (MDK2)	Z49085	
	-2.2	-1.7	phosphotyrosine protein phosphatase ACP1/ACP2	AA035993	E
	-2.0	-1.4	protein phosphatase type 1 (dis2m2)	M27073	
	-1.7	1.3	GTP-binding protein GTR1	Q00582	S
	-1.4	-1.4	preprosomatostatin	X51466	R, A
	-1.6	-2.6	L-glutamate decarboxylase (GAD)	M55253	R, A
	-1.4	-1.9	neurogranin / RC3	AA017811	R,E
	-1.5	-2.5	RAP1 GTPase activating protein (RAP1GAP)	W86617	E
	-1.5	-2.5	neuronal cannabinoid receptor (CB1)	U22948	
	-2.9	-3.5	alpha-2 adrenergic receptor	M97516	A
	2.4	-1.1	G25K GTP-binding protein GP (cdc42 homolog)	W59479	I,E
	-1.1	1.8	adenylyl cyclase, type VII	U12919	
			Ion Channels		
	-1.2	-1.7	voltage-dependent calcium channel beta-3 subunit	U20372	
	-1.2	-2.0	brain potassium channel protein-1 (MBK-1)	Y00305	
			Transcription		
	-1.8	-1.6	Id4 helix-loop-helix protein	X75018	
	-1.4	-2.4	retinoid X receptor gamma (RXR-gamma)	X66225	R, A
	1.8	-1.5	Hox-3.2	X55318	R
	-1.1	-1.6	brain factor-1	U36760	
	1.6	1.0	myelin gene expression factor (MEF-2)	U13262	
	3.3	2.2	NF-kappa-B DNA binding subunit	M57999	
	1.0	1.9	cerebral cortex transcriptional regulator T-Brain-1	U49251	
			Stress or Inflammatory Response		
	-1.3	-1.4	leukocyte neutral protease inhhibitor (LNPI)	AA145127	E
	-1.2	1.0	heat shock cognate 71 kD protein	P19378	S
	-1.8	1.1	macrophage inflammatory protein-1-beta	W67046	E
	1.7	1.2	DBA/2J delta proteasome subunit gene	U13393	
	2.2	2.2	rotamase (cyclophilin A)	AA060550	I,E
	1.5	1.4	heat shock cognate 71 kD protein	AA114576	R,E
	-1.2	2.1	cathepsin S precursor	AA146437	E
	1.5	1.8	apolipoprotein D	L39123	I
	1.1	3.2	proteasome activator PA28 alpha subunit	U60328	I
			Cell Cycle		
	-2.7	1.2	growth arrest DNA damage inducible protein 45	L28177	I
	-1.4	1.4	bcl-x transmembrane deleted (bcl-x long)	U10102	
	3.9	1.6	primase large subunit	D13545	
			Cytoskeleton and Cell Adhesion		
	-3.5	-1.3	ankyrin B, brain variant 2	AA153265	E
	-1.6	-1.1	neural cadherin	M31131	R
	-1.7	-1.1	connexin 30	Z70023	
	-1.4	-1.5	alpha-tubulin isotype M-alpha-4	M13444	
	-1.7	-1.7	thrombospondin 3 (Thbs3)	L04302	R
	-3.1	-1.4	myosin V	M33467	E
	-1.3	-2.3	myosin I	L00923	
	-1.4	-2.3	laminin receptor	J02870	
			Metabolism		
	-2.1	1.0	PC-1 nucleotide pyrophosphatase (NPPase)	AA103282	E
	-1.7	1.0	carbonic anhydrase isozyme II	K00811	
	-2.1	1.2	citrate transport protein	AA023087	E
	-1.6	-1.3	stearoyl-CoA desaturase (SCD2)	M26270	
	-1.8	-1.3	myo-inositol-1 (or 4)-monophosphatase	AA124192	E
	-1.7	-1.5	gamma enolase (neural enolase)	W48081	R, A, E
	-1.1	-1.8	lipoprotein lipase	M60847	
	-1.1	2.3	inositol polyphosphate 1-phosphatase	U27295	
	1.0	1.5	spermidine/spermine N1-acetyltransferase	L10244	
			Miscellaneous		
	-1.8	-1.9	pentylenetetrazol-related gene PTZ-17 (P311)	X70398	
	-1.5	-1.1	apolipoprotein E precursor	AA038067	E
	-1.6	1.0	similar to DEAD box protein RB	W13878	E
	-1.5	-1.9	N-glycan alpha-2,8-sialyltransferase	X83562	
	-2.3	1.3	probable phosphoserine aminotransferase	P10658	S
	-2.9	-1.6	putative regulatory protein TSC-22 (GILZ)	AA097366	E
	-2.1	-2.8	FISP-12	M70641	
	-1.2	-2.1	unknown	W84167	E
	-1.5	-2.1	seizure-related product 6 type 3 precursor	D29763	
	-1.4	-2.1	ADP-ribosylation factor-like protein 3 (ARD3)	W77226	E
	-1.1	-2.3	L1Md-9 repetitive sequence	M29325	
	2.7	-1.2	amyloid-like protein 1 precursor (APLP)	W82304	E
	2.2	1.5	thymosin B4 (Ptmb4)	W41883	E
	2.0	2.1	Ran/TC4 binding protein (RanBP1)	X56045	
	2.0	1.5	thioredoxin-dependent peroxide reductase	X82067	
	3.7	1.9	uterine mRNA	U38981	
	1.5	1.7	thioredoxin	W08120	R,E
	1.7	1.8	vacuolar ATPase subunit A gene	U13837	
	1.4	1.7	cytochrome c oxidase subunit VIIa	W91222	E
	1.7	1.6	NAP22	AA031158	E
	1.0	2.1	CIRP Cold inducible RNA-binding Protein	D78135	
	1.0	2.0	fibrillarin	Z22593	

*Difference Call and Fold Change are described in Methods. For sake of comparison, Fold Change is reported for both ages and bold faced only for samples that met criteria to be called "increased" or "Decreased".
"6 w" and "12 w" refers to 6- and 12-week time points, respectively. Difference Calls are represented as follows:
Blue = Decrease called in 4 of 4 comparisons of R6/2 to control. Red = Increase called in 4 of 4 comparisons. Light Blue = Decrease called in 3 of 4 comparisons. Light Red = Increase called in 3 of 4 comparisons.
Notes: R = retinoid-responsive genes/proteins, I = interferon-responsive genes, A = cAMP-responsive genes/proteins, E = EST, S = EST sequence similar to named gene & genbank number.
Retinoid references: (9-20) and references within. Interferon data from S. Der and B. Williams, personal communication. cAMP references: (21-28) and references within.

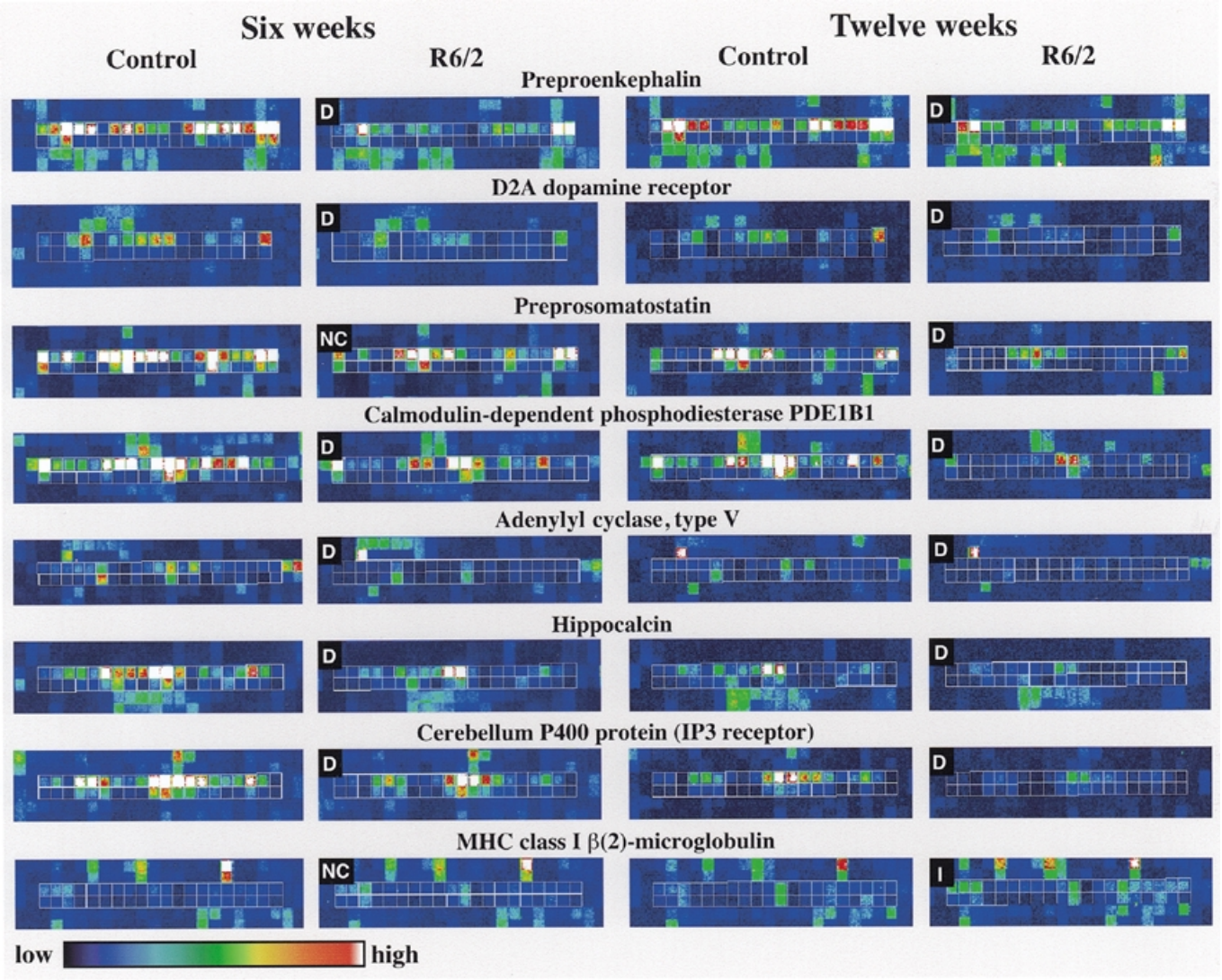

Figure 1. Primary microarray data. Each panel represents the microarray hybridization signal for a pooled wild-type or R6/2 mouse sample. The 20 probe tilings for each differentially detected mRNA are outlined in white. Within each outlined region, the top row of probes is comprised of oligonucleotides that are perfect sequence complements to the RNA of interest. The second row is comprised of control oligonucleotides, each of which differs from the perfectly matched probe tiled above it by a single base substitution. Difference calls are represented in the R6/2 panels by the following abbreviations: D, decrease in R6/2 relative to wild-type; I, increase in R6/2 relative to wild-type; NC, no change in R6/2 relative to wild-type. The pseudo-color hybridization scale is shown at the bottom of the figure.

(e.g. glial fibrillary acidic protein, myelin basic protein or major histocompatability complex II components) were observed. Likewise, some mRNAs known to be expressed in medium spiny neurons (e.g. preprotachykinin) were unchanged. These findings indicate that decreases in the expression of neuronal signaling genes are not due to large shifts in striatal cell populations.

While many components of signaling cascades implicated in human HD were obviously changed in R6/2 brains, some mechanisms previously associated with the disease were represented only minimally. For example, very few changes were detected in mRNAs that encode mitochondrial proteins, proteolytic enzymes or apoptotic molecules. This may be due to their regulation by post-transcriptional mechanisms. Alternatively, these HD-related toxicities may be modest, and thus undetectable, at the R6/2 time points selected.

At 12 weeks, R6/2 animals are diabetic, showing both elevated baseline glucose levels and abnormal glucose tolerance tests, whereas 6-week-old animals handle glucose normally by these criteria (ref. 34; O. Andreasson and M.F. Beal, personal communication). Changes in mRNAs associated with glucose metabolism were not prominent in R6/2 mice at either age. Specifically, no differences in mRNAs, including glyceraldehyde phosphate dehydrogenase, glucose 6-phosphate isomerase, 6-phosphofructokinase, fructose bisphosphate aldolase, pyruvate dehydrogenase, phosphoglycerate kinase, lactate dehydrogenase and triose phosphate isomerase, were detected between R6/2 mice and controls. These data indicate that diabetes in R6/2 mice does not obscure the detection of bona fide huntingtin fragment-induced changes in gene expression.

Increased expression of genes associated with inflammation

Of over 6000 mRNAs represented on the microarrays, only 22 were increased in 6-week-old R6/2 mice and 21 were increased in 12-week-old mice compared with controls. In contrast to the mRNAs that were decreased in R6/2 mice, the increases in gene expression were generally not concentrated in discrete functional categories. The possible exceptions were mRNAs that encode stress or inflammation mediators and the expression of genes associated with cell cycle regulation. mRNAs increased at 6 weeks included rotamase/cyclophilin A and immunophilin P59. The proteins encoded by these mRNAs regulate the function of calcineurin, ryanodine receptors and phosphatidylinositol triphosphate (IP_3) receptors (see Calcium homeostasis and mobilization above) and are inhibited by immunosuppressants such as cyclosporin and FK506. At the 12-week time point cathepsin S, apolipoprotein D and MHC β2 microglobulin mRNAs were increased. These mRNAs are also induced in a mouse scrapie model, which represents another 'protein aggregation' disease (35). Several inflammation-related mRNAs and other mRNAs that are increased in R6/2 mice were induced by interferon-α in mouse primary fibroblasts assayed on Mu6500 microarrays (Tables 1A and 1B; S. Der and B. Williams, personal communication). Whether these mRNAs can be coordinately regulated in R6/2 mice by immune mediators remains to be determined.

Confirmation of microarray findings

In order to confirm changes in mRNA expression detected by the microarrays and to extend our understanding of the anatomical distribution of these changes, we performed northern blotting and *in situ* hybridization histochemistry (ISHH) experiments using independent litters of R6/2 mice. Northern hybridization results correspond to the array data for three decreased genes (zif268, GIR and PCTP), one unchanged gene (NMDA-NR1) and two increased genes ($G\gamma_3$ and PA28α) in R6/2 mice (Fig. 2). mRNAs were also measured in brain tissue sections by ISHH (Fig. 3). We confirmed striatal decreases for six mRNAs at 6 and 12 weeks and striatal increases in two mRNAs at 12 weeks by this method. These studies confirmed the array data with regard to differences in expression levels and provided anatomical resolution in the striatum and cortex. Cortical decreases in junB, N10 and zif268 at 6 and 12 weeks and cortical increases in $G\gamma_3$ and PA28α at 12 weeks were observed.

Striatal gene expression profiles from 6-week-old R6/2 mice were directly compared with those from 12-week-old animals to determine whether there were changes indicative of disease progression (analysis not shown, refer to www.neumetrix.com). While many genes in both R6/2 animals and controls differed between the two time points, certain mRNAs characteristic of mature medium spiny neurons, such as preproenkephalin, dopamine D_2 receptors and glutamic acid decarboxylase, decreased as neurological symptoms progressed. This was confirmed by the ISHH data for preproenkephalin and DARPP-32, another mRNA characteristic of this cell population (ref. 36 and Fig. 3). Previous ISHH assays have also shown progressive decreases in adenosine A_{2a} and dopamine D_1 and D_2 receptor mRNAs (3,4).

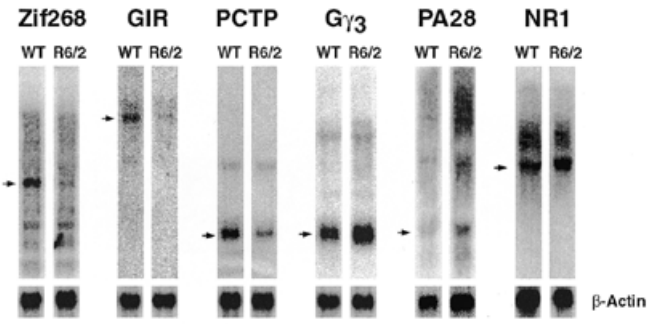

Figure 2. Northern analysis of genes called differentially expressed in 12-week-old R6/2 mice by microarray analysis. Representative northern autoradiograms show expression in wild-type (WT) versus R6/2 animals. After subtraction of background, hybridization signals were normalized to that of β-actin (n = 2 for PA28α, n = 3 for all others). Ratios of mean values are as follows: zif268, R6/2 = 21% control (34% by microarray at 12 weeks); GIR, 54% control (23% control by microarray at 12 weeks); PCTP, 77% control (17% control by microarray at 12 weeks); heterotrimeric G-protein subunit $G\gamma_3$, 145% control (240% by microarray at 12 weeks); proteasome activator subunit PA28α, 269% control (320% by microarray at 12 weeks by moderate stringency criteria); NMDA-NR1, 89% control (no microarray calls at 12 weeks). Arrows indicate bands of interest [signals correspond to the following RNA lengths, as estimated by electrophoretic mobility relative to rRNA: zif268, 2.5 kb; GIR, 6 kb; PCTP, 1.3 kb; $G\gamma_3$, 1.2 kb; PA28, 1.0 kb (upper bands represent related members of the PA28 complex); NR1, 4 kb; β-actin, 1.0 kb].

Type II and V adenylyl cyclases were decreased whereas type VII adenylyl cyclase was increased in the microarray analysis. To determine the overall impact on adenylyl cyclase levels, [^{3}H]forskolin binding assays were performed. [^{3}H]forskolin binds to all adenylyl cyclase subtypes and provides a measure of adenylyl cyclase protein levels. [^{3}H]forskolin binding was decreased in R6/2 striata to 24% of wild-type in 12-week-old animals (P = 0.0053, n = 5).

Signaling molecules affected in R6/2 mice are also decreased in other HD transgenic mice

The comparisons of R6/2 data to littermate controls demonstrated that the presence of the expanded repeat *IT15* exon 1 transgene resulted in the mRNA changes described above. To determine the extent to which these changes might be specific to this mouse model, we examined the expression of a subset of these mRNAs in another line of HD transgenic mice, N171-82Q (mice described in Materials and Methods and ref. 37). Significant decreases in symptomatic 4-month-old N171-82Q mice relative to N171-18Q or wild-type mice were observed in binding assays for dopamine D_2 receptors (78% control), adenosine A_{2a} receptors (61% control) and adenylyl cyclase (71% control) and *in situ* hybridization for D_2 (61% control), N10 (49% control), preproenkephalin (59% control) and DARPP-32 (62% control) (Table 2). ISHH for junB, $G\gamma_3$ and zif268 was not different from controls (n = 3). Differences between the findings in R6/2 and N171-82Q lines could arise from differing polyglutamine lengths, promoters, transgene insertion sites or mouse strains. Overall, the concordance between microarray, northern, *in situ* and binding analyses performed on independent litters of mice from the two transgenic lines suggest that gene expression changes are characteristic of HD pathogenesis (see below).

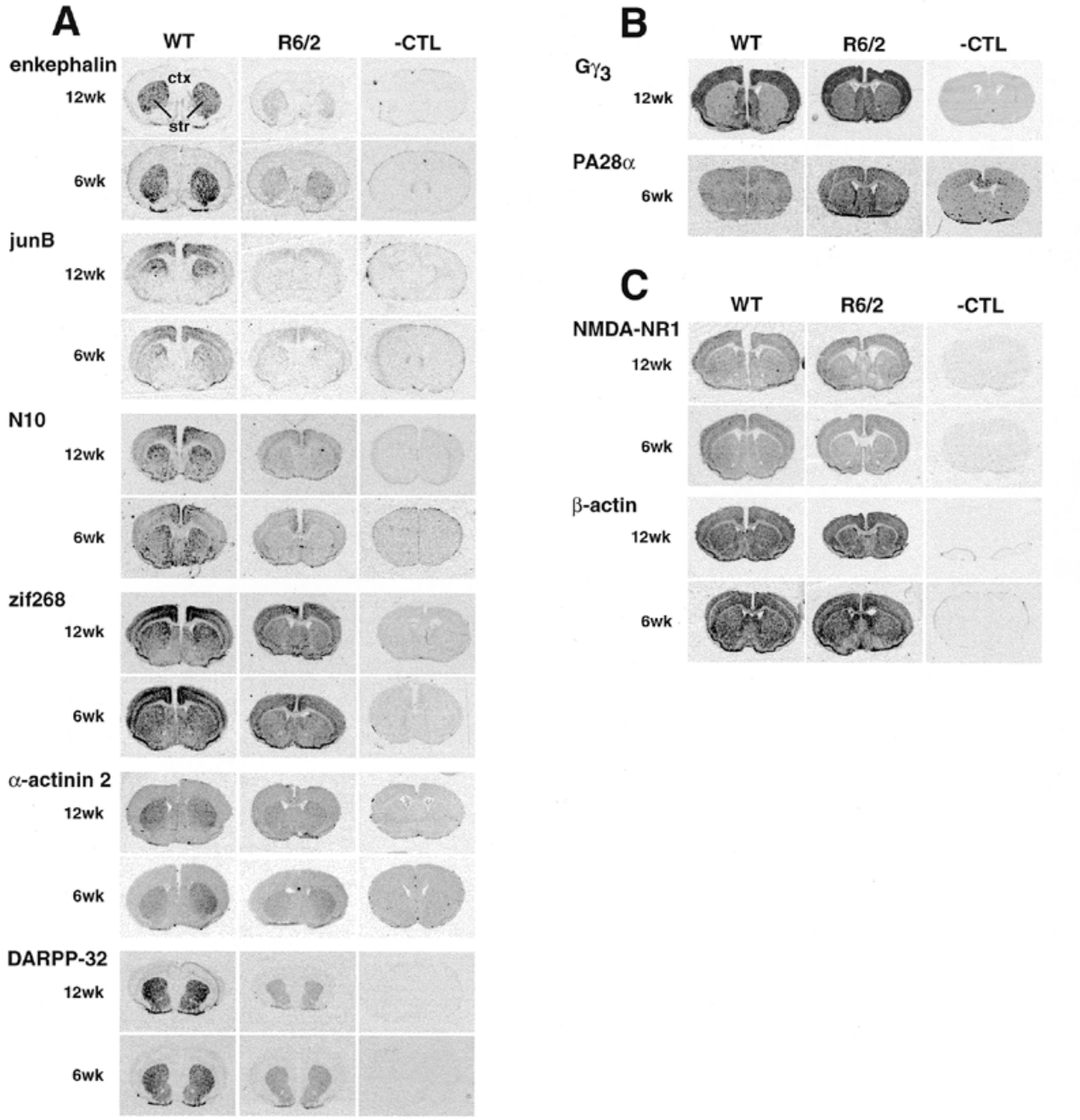

Figure 3. *In situ* hybridization histochemistry of genes differentially expressed in wild-type (WT) and R6/2 mice. Representative film autoradiograms show the anatomical resolution of hybridization signals for differentially expressed mRNAs in the striatum and cerebral cortex. Negative control panels (–CTL) represent hybridization to sense strand cRNA probes or labeled oligonucleotide hybridization in the presence of a 200-fold excess of unlabeled oligonucleotide. (**A**) Genes showing decreased expression in 6- and 12-week-old R6/2 mice [with percent controls calculated from mean optical densities (MODs) after subtraction of film background and sense cRNA MODs where applicable, unless otherwise indicated]: preproenkephalin (21% control striatum 12 weeks, 30% control striatum 6 weeks) zif268 (55% control striatum 12 weeks, 66% control cortex 12 weeks, 66% control striatum 6 weeks, 82% control cortex 6 weeks); junB (21% control striatum 12 weeks, 39% control cortex 12 weeks, 37% control striatum 6 weeks, 59% control cortex 6 weeks); N10 (50% control striatum 12 weeks, 58% control cortex 12 weeks, 50% control striatum 6 weeks, 72% control cortex 6 weeks); α-actinin 2 (70% control striatum 12 weeks, 72% control striatum 6 weeks); DARPP-32 (dopamine and cyclic AMP-regulated phosphoprotein, relative molecular mass 32 000) (33% control striatum 12 weeks, 54% control striatum 6 weeks). (**B**) Genes showing increased expression in 12-week-old R6/2 mice: PA28α (128% control striatum 12 weeks, 130% control cortex 12 weeks; percent control calculated from MOD film background); $G\gamma_3$ (617% control striatum 12 weeks, 130% control cortex 12 weeks). (**C**) Genes showing unaltered expression in 6- and 12-week-old R6/2 mice: NMDA-NR1 (96% control striatum 12 weeks, 104% control striatum 6 weeks), β-actin (94% control striatum 12 weeks, 112% control cortex 12 weeks, 88% control striatum 6 weeks, 100% control cortex 6 weeks). Percentages of control and MODs represent the fraction of hybridization signals from four R6/2 and four wild-type animals.

Table 2. Summary of signaling pathway changes in N171-82Q mice and comparison to R6/2 mice

mRNA/protein	N171-82Q mice at 4 months of age				R6/2 mice at 12 weeks of age (% control)			
	Percent control	*P*-value	Assay	*n* (control, N171-82Q)	Binding	ISHH	Northern	Array
Dopamine D_2 receptor	78	0.0290	Binding	8, 6	50[a]	66[b]		38
Adenosine A_{2a} receptor	61	0.0027	Binding	8, 6	10[b]	68[b]		No change detected
Adenylyl cyclase	71	0.0003	Binding	8, 6	24			Multiple changes
Dopamine D_2 receptor	61	0.0032	ISHH	3, 3	50[a]	66[b]		38
N10	49	0.006	ISHH	3, 3		50		33
Preproenkephalin	59	0.013	ISHH	3, 3		21		45
DARPP-32	62	0.003	ISHH	3, 3		33		Not on array
JunB	67	0.478	ISHH	3, 3		21		32
zif268	93	0.673	ISHH	3, 3		56	21	34
Gγ3	112	0.710	ISHH	3, 3		617	145	240

[a]Data from Cha *et al*. (3).
[b]Data from Cha *et al*. (4).
Other data from current study.

Changes in gene expression in R6/2 brains parallel decreased mRNA and protein levels described in previous HD studies

It is important to consider whether the observed changes in steady-state mRNA populations in HD mouse models result in reduced protein levels and function and whether there is a link between mouse model data and human disease. In the present study, we addressed changes in protein levels in a limited fashion by demonstrating that forskolin binding was diminished in R6/2 mice and that binding to dopamine D_2 receptors, adenosine A_{2a} receptors and adenylyl cyclase was decreased in N171-18Q mice. Though extensive protein analysis was beyond the scope of this study, microarray-based mRNA findings were consistent with previous work that used both human tissue and mouse models of HD. Previous studies in our laboratory have shown decreases in A_{2a}, D_1 and D_2 receptor mRNAs and in corresponding protein levels based on receptor binding assays performed in three different lines of mice transgenic for a CAG-expanded exon 1 of the *IT15* gene (R6/1, R6/2 and R6/5) (3,4). In the HDex6 and HDex27 lines, which are transgenic for exon 1 of the human *IT15* gene containing 18 CAG repeats, striatal levels of A_{2a}, D_1 and D_2 binding and mRNA are equivalent to wild-type animals, indicating that the CAG expansion of exon 1 is necessary for their down-regulation (4). In addition, other researchers have shown that decreases in preproenkephalin mRNA are associated with decreased enkephalin immunoreactivity in R6/2 striata (38).

Parallels can also be found between decreased mRNAs in R6/2 striata and decreased mRNA and protein levels in human HD brains. Preproenkephalin mRNA is diminished in early stage human Huntington's disease brains (39,40). Human HD brains also show specific decreases in the enzymatic activities of neuron-specific enolase, protein kinase C isoform βII and glutamic acid decarboxylase (41–43). *In vitro* binding assays show decreases in IP_3 receptor, L-type calcium channel and cannabinoid receptor (42,44–46; see ref. 47 for cannabinoid ISHH data in R6/2 mice). Moreover, D_1 and D_2 dopamine receptor binding is decreased *in vitro* and *in vivo* in presymptomatic patients carrying the HD mutation (2). Although the subset of mRNAs in Table 1 that have been tested at the protein level is small, the results demonstrate that gene expression changes in the 6- and 12-week-old R6/2 striata mirror previously described changes in HD.

DISCUSSION

This study identified genes that were aberrantly expressed in the striata of R6/2 mice using an expression array that interrogates ~6000 mRNAs. This screen, while far from saturating, identified gene networks that are affected by the HD mutation. Our data suggest that the dysregulation of mRNAs encoding neurotransmitter receptors and related second messenger systems is an early component of the pathological process. In addition, a small number of mRNAs responsive to inflammatory mediators were increased. mRNAs encoding mitochondrial proteins, caspases and other apoptosis-related molecules, all of which have been implicated in HD, were relatively unaffected. mRNAs encoding neuronal structural proteins were also generally unchanged between experimental and control mice, consistent with histopathological observations that R6/2 mice have normal cell counts (33). Thus, RNA changes in these mice are not simply due to neuronal death.

Although we and others have previously demonstrated decreased expression of dopamine, glutamate and adenosine receptors in HD, this study demonstrates that many components of their signaling pathways and target genes are similarly reduced. In Figure 4, genes whose expression is altered by mutant huntingtin are integrated into a schematic drawing of a striatal medium spiny neuron, demonstrating the extent to which signal transduction genes are affected. Reduced levels of neurotransmission-regulated immediate early gene mRNAs and adenylyl cyclase protein suggest that, overall, mutant huntingtin-mediated mRNA changes impair transduction of neuron-specific signals. Whether this is an adaptive response of neurons to mutant huntingtin remains to be determined. In

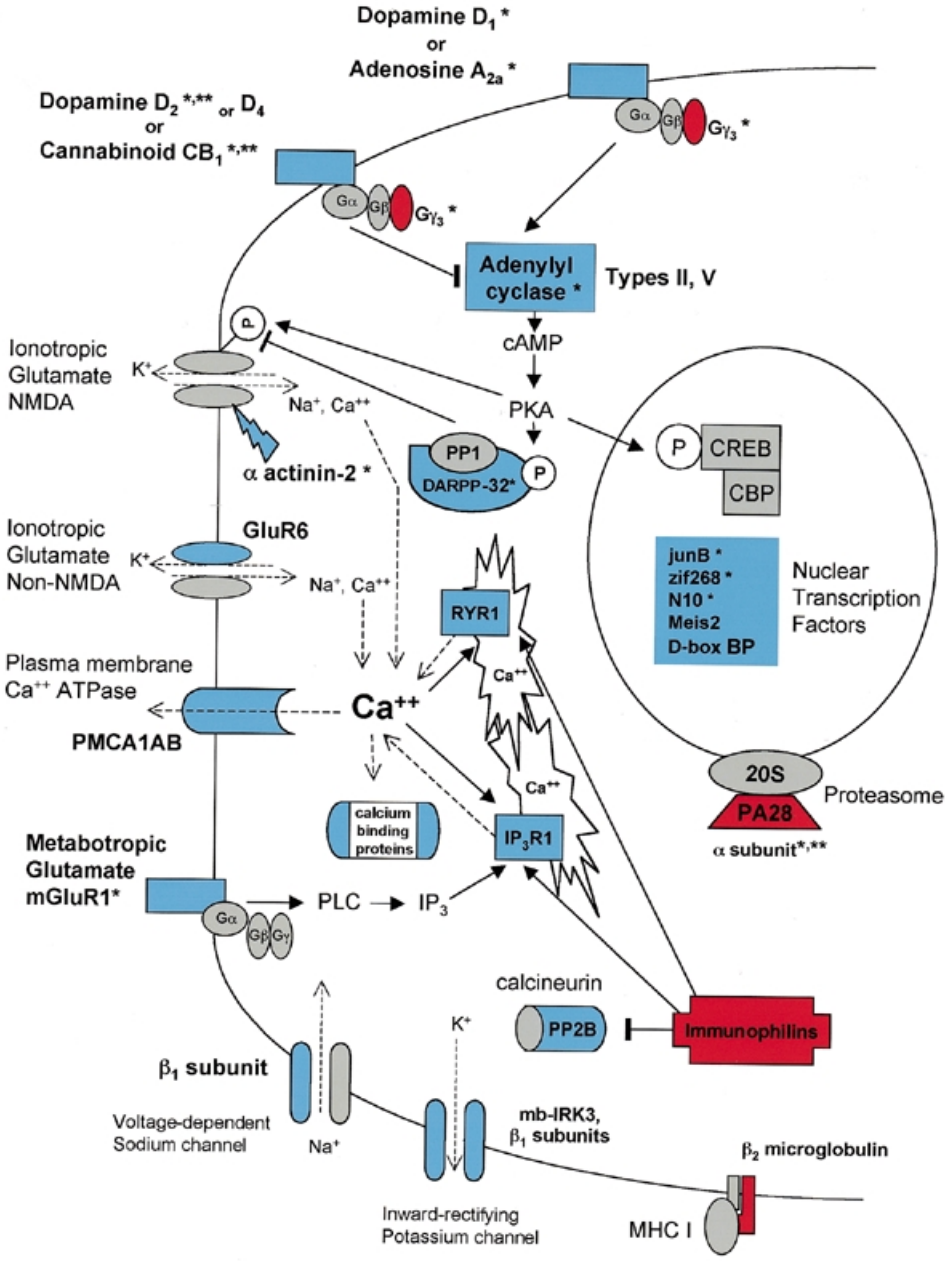

Figure 4. Functional relationships of products of differentially expressed genes in striatal medium spiny neurons. Bold type indicates products of differentially expressed mRNAs called in four of four GeneChip comparisons (Table 1A) or confirmed independently by another method (single asterisk). The color of each element represents the direction of the change; red elements are increased, blue elements are decreased and gray elements are either unchanged, did not meet the above criteria or have not been examined. Plain lines with triangular arrows represent sequential events or positive regulation; blunt bars represent negative regulation. Hatched arrows represent the flow of ions. Double asterisks indicate mRNAs detected as differentially expressed using medium stringency criteria. For the sake of presentation, only representative members of the protein phosphatase 1/DARPP-32 regulatory pathway are shown; a thorough review of this pathway can be found elsewhere (36).

addition to the decreased messages encoding afferent signaling molecules, decreased expression of preproenkephalin and glutamic acid decarboxylase suggests that medium spiny neurons may generate abnormally decreased efferent signals.

The array data further demonstrate abnormal expression of multiple genes involved in calcium signaling, consistent with studies in another mouse HD model that showed increased basal calcium levels and decreased glutamate-induced calcium mobilization (31). The mRNA profiling in our study indicates that elevated basal calcium could be attributed to a diminution of plasma membrane calcium ATPase activity. Also, losses of mRNAs encoding IP_3 and ryanodine receptors, voltage-sensitive calcium channels, calcium-binding proteins, and calcium/calmodulin-dependent enzymes could prevent the generation of appropriate calcium-mediated intracellular signals in response to glutamate. The blunting of calcium-mediated

responses through all of these mechanisms could cause deficits in many important neuronal functions, including synaptic plasticity.

Both microarray and ISHH demonstrate that gene expression changes occur in minimally symptomatic animals and persisted during progression of the disease in R6/2 mice. This suggests that disease progression might represent the accumulation of neuronal damage caused by a persistent dysregulation of signaling systems. It has been shown that long-term potentiation (LTP) and long-term depression (LTD) deficits occur in transgenic models of HD, including R6/2 mice (ref. 31; K. Murphy, personal communication). The array data showed decreased expression of many of the mediators of LTP and LTD, such as cyclic AMP cascades, calcium-dependent kinases and phosphatases, voltage-dependent calcium channels and glutamate receptors. The notion that deficits in neurotransmission occur early in disease progression is supported by human PET studies reporting losses of D_1 and D_2 receptors in clinically asymptomatic HD gene-positive individuals (2).

This study also provides the first evidence that impaired retinoid signaling might contribute to HD pathophysiology. In addition to decreased RXRγ, retinoic acid signaling regulates at least 22 of the 104 genes that show decreased expression in R6/2 mice. The disruption of RA signaling by mutant huntingtin can be explained by either of two mechanisms: first, dopamine can positively regulate the expression of retinoic acid receptor genes and the diminished activity of the dopamine signaling pathway in HD might decrease RXRγ expression (10); second, the nuclear co-repressor NCoR binds both mutant huntingtin and retinoic acid receptors (7,11) and could sequester receptors in a non-functional complex. It is interesting to note that glial cells in the lateral striatum produce more retinoids than those in the medial striatum, resulting in a concentration gradient across the structure that is opposite to the gradient of neural degeneration in HD (12). In other words, the striatal neurons that degenerate first in HD are those surrounded by the lowest concentration of retinoids.

The signaling pathways affected by the mutant huntingtin protein represent logical targets for therapeutic intervention. The current data indicate a potential therapeutic role for drugs that restore neuronal calcium homeostasis, modulate dopamine or glutamate signaling pathways or that inhibit inflammatory responses. Because retinoic acid analogs have been clinically demonstrated to overcome retinoic acid receptor deficits (e.g. in acute promyelocytic leukemia; ref. 48), it is possible that the deficits in HD striatal neuron retinoic acid receptors and binding proteins could be compensated for by pharmacological doses of retinoic acid agonists. The identification of a distinct gene expression signature in the striata of R6/2 mice provides a valuable reference for the rapid assessment of therapeutic efficacy in candidate drug screens.

MATERIALS AND METHODS

Animals

Female R6/2 mice (33) and wild-type controls (F1) were purchased from The Jackson Laboratory (Bar Harbor, ME) and killed at 5–6 or 11–12 weeks of age. R6/2 mice express exon 1 of the human *IT15* gene containing an extremely expanded CAG repeat (140–147) under control of the human *IT15* promoter. These animals appear to develop normally through weaning, but display subtle deficits starting at 5–6 weeks of age which progress to a resting tremor, involuntary movements, stereotypic grooming and handling-induced seizures by 9–12 weeks of age (33,49).

N171-82Q mice and controls (N171-18Q and wild-type) (37) were obtained from the authors' colony (G.S., C.A.R. and D.R.B.) and killed at 4 months of age (late symptomatic stage for the N171-82Q mice). The N171 mice used for the present study carry a transgene encoding the N-terminal 171 amino acids of human huntingtin with a polyglutamine repeat length of 18 (N171-18Q) or 82 (N171-82Q), expressed under the control of the PrP promoter. Phenotypically, N171-82Q animals show loss of coordination, tremors, hypokinesis, gait abnormalities and premature death (37).

Gene expression changes in R6/2 and N171-82Q mice are attributable to an N-terminal portion of the human huntingtin protein expressed from a partial *IT15* transgene. There are several lines of evidence to support the relevance of a similar mutant huntingtin fragment to the human disease. First, a similar proteolytic fragment of huntingtin has been detected in human HD brains and those of several HD models (32,50). Second, such a fragment has a higher propensity for aggregation (50,51) and appears to be present in huntingtin-positive aggregates in human brain (52). Additionally, this fragment contains structural domains that mediate most of huntingtin's known protein–protein interactions (7,53,54).

Tissue

For RNA extractions, the striata were dissected bilaterally, removed immediately to dry ice and stored at –70°C until the tissue was processed. For *in situ* hybridization histochemistry and autoradiographic studies, brains were frozen whole by immersion in isopentane on dry ice for 3 min, then stored at –70°C until the tissue was sectioned. Cryostat sections (12 µm) containing striatum and cortex were thaw mounted onto polylysine-coated glass slides.

RNA extraction

RNA was extracted using TRI-Reagent (Sigma, St Louis, MO) according to the manufacturer's recommended protocol, except that the isopropanol precipitation step was performed at –20°C overnight. RNA pellets were resuspended in nuclease-free water and quantitated spectrophotometrically.

Preparation of labeled cRNA

RNA from the striata of six R6/2 or six age-matched wild-type animals at each age was combined to comprise each sample, consisting of 70–100 µg of total RNA. Poly(A)$^+$ RNA was isolated from the samples using Oligotex mRNA isolation kits (Qiagen, Chatsworth, CA). At this point the samples were split in half and all further procedures were performed on each pool independently. Biotinylated cRNAs were prepared per Affymetrix protocol. Labeled cRNA (32 µg) was fragmented in 40 µl of 40 mM Tris–acetate pH 8.0, 100 mM KOAc, 30 mM MgOAc for 35 min at 95°C. The fragmented cRNA was brought to a final volume of 300 µl in hybridization buffer containing 100 mM MES, 20 mM EDTA, 0.01% Tween-20 (all from Sigma), 1 M NaCl (Ambion, Austin, TX), 0.5 mg/ml

acetylated BSA (Gibco BRL, Gaithersburg, MD), 0.1 mg/ml herring sperm DNA (Promega, Madison, WI) and biotinylated controls B2, BioB, BioC, BioD and Cre (Affymetrix, Santa Clara, CA) at 50, 1.5, 5, 25, 100 pM, respectively.

Array hybridization

Mu6500 A, B, C and D oligonucleotide arrays were prehybridized, hybridized, washed and stained as recommended by the manufacturer (Affymetrix) using a GeneChip Fluidics Station 400 (Affymetrix). The arrays were hybridized sequentially over the course of 4 days using 200 µl of cRNA (0.1 µg/µl) per hybridization. After hybridization of one array, the aliquot was recovered from the array, recombined with the unused portion of the sample and frozen. This process was repeated with each sample until the sample had been hybridized to the entire set of four arrays. Immediately after washing and staining, the probed arrays were scanned with a Hewlett Packard GeneArray scanner. The scanned images were analyzed and compared using GeneChip3.1 software (Affymetrix) (8). Images were globally scaled to compensate for minor variations in fluorescence and bring the mean average difference for all of the genes on each array to 2500 intensity units.

Criteria for selecting affected genes

We designed our study to minimize potential experimental confounds as follows. First, we used a pooled sample for the Affymetrix GeneChip analysis, followed by validation in independent litters of mice in order to minimize effects of animal-to-animal and litter-to-litter variability. Second, we analyzed each sample in duplicate, to control for differences in efficiency of mRNA amplification and chip variability. Third, we confirmed a subset of our findings by other methodologies and in other lines of HD transgenic mice.

We compared each R6/2 sample to both age-matched control samples, thus for each age of mice obtaining four mutant to wild-type comparisons. We used the default parameters in the GeneChip3.1 software to call mRNAs increased, decreased or not changed in the R6/2 striata relative to the controls. No additional thresholds (e.g. minimum fold change) were introduced. The GeneChip3.1 Difference Call Decision Matrix (8) is a metric based on the magnitude and sign of the hybridization signal difference between the two samples being compared plus a tallying of the various oligonucleotide probes that have a positive or negative signal change. Typically, the genes on the arrays are represented by an average of 20 probe pairs. mRNAs that were called as increased or decreased in at least three of the four comparisons were designated for inclusion in this report. This cut-off was chosen based on the following considerations: (i) prior findings show a >90% concordance between Affymetrix microarray data and northern/S1 protection assay data in studies of similar design (J.M. Olson, A. Strand and S.J. Tapscott, unpublished observations); (ii) comparison of two hybridizations of the same sample yields a call rate <1% (which can be considered an estimate of the 'false positive' rate). Thus, the representation of mRNAs called in three of four comparisons at a false positive rate of up to 1% is extremely low. Table 1 lists genes that differed between R6/2 and wild-type striata in 4/4 (high stringency) and 3/4 (moderate stringency) comparisons and the entire data set is available at www.neumetrix.com . As mentioned above, the persistent expression of genes in cells not affected by mutant huntingtin serves to reduce the apparent magnitude of any changes. A less stringent examination of the data that relies solely on the probe pairs is also presented at www.neumetrix.com

Probes for *in situ* and northern hybridization

Probe sequences used for *in situ* and northern hybridization were cloned by RT–PCR, obtained as I.M.A.G.E. Consortium clones (from Genome Systems, St Louis, MO) or ordered as custom oligonucleotides (from Gibco BRL). Oligonucleotide primers and probes were either designed (those listing GenBank accession nos) using Oligo 4.06 software (National Biosciences, Plymouth, MN) and analyzed for specificity by database searching using BLASTN (National Center for Biotechnology Information, Bethesda, MD) or selected based on use in previous studies. T7 and SP6 promoter sequences (CTGTAATACGACTCACTATAGGG and GGGATTTAGGTGACACTATAGAA, respectively) were added to the 5′-ends of PCR primers in some cases for use in *in vitro* transcription of riboprobes. Gene-specific sequences of primers used to clone probes by RT–PCR were as follows: α-actinin 2 (GenBank accession no. AA800206), CGTAGAGGGCAGGAGAAG and TTTGACAGGAGGAAGAATGG; NMDA-NR1, GGAGTGGAACGGAATGATGG and AAAGCCTGAGCGGAAGAACA (outer) and CTGTAATACGACTCACTATAGGGTTATGCAGCCTTTTCAGAGC and GGGATTTAGGTGACACTATAGAAGCACGGCCGAGTCCCAGAT (inner); zif268 (GenBank accession no. M22326), GTTCGGCTCCTTTCCTCACT and GCCTCTTGCGTTCATCACTC (outer) and TGAAGAAGGCGATGGTGGAGA and GGCAGAGGAAGACGATGAA (inner). PCR-generated probe templates were purified using a Strataprep PCR Purification Kit (Stratagene, La Jolla, CA). The following *in situ* probes were obtained as I.M.A.G.E. Consortium clones: GIR (ID 421187); $G\gamma_3$ (ID 47893); PA28α (ID 598746). Oligonucleotide *in situ* probes comprised: DARPP-32 (GenBank accession no. U23160), GAGCTGGCTCGGGGGCGCGGGCACAGAGAA; junB, ACTGGGCGCAGGCGGGCGGGCCGGAGTCCAGTGTGTGAGCTGCGCC; N10, GTGGTCACGCGGTCCTGGGCTCGTTGCTGGTGTTCCATATTGAGC; β-actin, GCCGATCCACACGGAGTACTTGCGCTCAGGAGGAGCAATGATCTT; preproenkephalin (GenBank accession no. M28263), ATCTGCATCCTTCTTCATGAAACCGCCATACCTCTTGGCAAG GATCTC. Probes used for the following northern blots were generated by PCR subcloning partial I.M.A.G.E. Consortium clone sequences: PA28α (primers AGAAGAAAGGGGACGAAGAC and TGTTTGGGAGGCAGAGTGAG); $G\gamma_3$ (primers CTCCCCACTGACCCTACATC and CTGCCTTGGACACCTTTATC); GIR (primers TGACAGCTATCGCAGTGGAC and CAGCAGAGGGCAAAGAGGAC). The identities of PCR products and I.M.A.G.E. Consortium clones were confirmed by sequencing.

Northern analysis

Two micrograms of each RNA sample were denatured in 1× MOPS containing 50% formamide and 3% formaldehyde, electrophoresed through a 1.2% agarose gel containing 3% formaldehyde and electorphoretically transferred to a nylon membrane. Random primed ^{32}P-radiolabeled cDNA probes (sp. act. ~6.0×10^9 d.p.m./µg) were prepared using a Prime-It kit (Stratagene). Oligonucleotide probes were labeled using the

Renaissance oligonucleotide 3′-end-labeling system (NEN Life Sciences). Hybridization took place overnight at 42°C, and final high-stringency washes were performed with 0.5× SSC (for oligonucleotide probes) or 0.1× SSC (for cDNA probes) plus 0.1% SDS at 42°C. Hybridization was detected by autoradiography using a Molecular Dynamics PhosphorImager (Sunnyvale, CA) and the signal was quantitated using ImageQuant software (v.1.2).

In situ hybridization histochemistry

PCR products and I.M.A.G.E. clones (above) were used as templates for *in vitro* transcription of ^{35}S-labeled riboprobes. Oligonucleotide probes were prepared using the Renaissance oligonucleotide 3′-end-labeling system and purified with NENsorb columns (NEN Life Sciences). ISHH was conducted according to Landwehrmeyer *et al*. (55) (cRNA probes) or Augood *et al*. (56) (oligonucleotide probes) with 12 µm fresh-frozen cryostat sections of mouse brain. Autoradiograms were obtained on Hyperfilm β-Max (Amersham, Arlington Heights, IL) by 2–28 day exposures. Films were developed and analyzed using a computer-based image analysis system (M1; Imaging Research, St Catharine's, Ontario, Canada).

Receptor and adenylyl cyclase autoradiography

All studies were performed on coded samples by experimenters blinded to the genotype status of the animals. Dopamine D_1 and D_2 receptor assays used a buffer containing 25 mM Tris–HCl pH 7.5, 100 mM NaCl, 1 mM $MgCl_2$, 1 µM pargyline and 0.001% ascorbate. For D_1 receptors, slides were incubated with 1.65 nM [^{3}H]SCH-23390 (sp. act. 70.3 Ci/mmol; NEN Life Sciences) for 2.5 h. Non-specific binding was defined in the presence of 1 µM *cis*-flupentixol (57). For D_2 receptors, slides were incubated with 180 pM [^{3}H]YM-09151-2 (sp. act. 85.5 Ci/mmol) for 3 h. Non-specific binding was defined in the presence of 50 µM dopamine (58). For adenosine A_{2a} receptors, the buffer used was 50 mM Tris–HCl, pH 7.4 with 10 mM $MgCl_2$. Following a preincubation for 30 min at room temperature in buffer containing 2 IU/ml adenosine deaminase, slides were incubated in buffer containing 5 nM [^{3}H]CGS 21680 (sp. act. 39.5 Ci/mmol) for 90 min (59). Non-specific binding was defined in the presence of 20 µM 2-chloroadenosine. Slides were rinsed for 5 min in ice-cold buffer, then quickly in ice-cold ddH_2O and dried rapidly under a stream of warm air. For adenylyl cyclase, slides were incubated in 10 nM [^{3}H]forskolin in 50 mM Tris–HCl with 100 mM NaCl and 5 mM $MgCl_2$ for 10 min at room temperature (60). Slides were rinsed twice for 2 min at 4°C and then dried. Slides were apposed to tritium-sensitive film (Hyperfilm ^{3}H; Amersham) with calibrated radioactive standards and exposed for 1–3 weeks. Films were developed and analyzed using a computer-based image analysis system (M1; Imaging Research). Image density corresponding to binding of [^{3}H]ligand was converted to pmol/mg protein using calibrated radioactive standards and non-specific binding was subtracted.

ACKNOWLEDGEMENTS

We are grateful to Jim Eberwine, Leslie Thompson, Sarah Augood and Jonathan Cooper for helpful discussions and critical evaluation of the manuscript. We also thank Jeff Delrow and colleagues in the DNA Microarray Laboratory at the FHCRC. This work was supported by the Hereditary Disease Foundation (R.L.-C., C.A.R., D.R.B., A.B.Y. and J.-H.J.C.), the Huntington's Disease Society of America (R.L.-C., C.A.R., D.R.B. and J.-H.J.C.), USPHS grants (NS10800 to R.L.-C.; NS16375 and NS38144 to C.A.R. and D.R.B.; AG13617 and NS38106 to A.B.Y.; NS01916 to J.-H.J.C; HD28834 to J.M.O. through the University of Washington Child Health Research Center), the Glendorn Foundation (A.B.Y.) the W.M. Keck Foundation and the Burroughs Wellcome Fund (Career Award to J.M.O.).

REFERENCES

1. Huntington's Disease Collaborative Research Group (1993) A novel gene containing a trinucleotide repeat that is unstable in Huntington's disease chromosomes. *Cell*, **72**, 971–983.
2. Weeks, R.A., Piccini, P., Harding, A.E. and Brooks, D.J. (1996) Striatal D_1 and D_2 dopamine receptor loss in asymptomatic mutation carriers of Huntington's disease. *Ann. Neurol.*, **40**, 49–54.
3. Cha, J.-H., Kosinski, C.M., Kerner, J.A., Alsdorf, S.A., Mangiarini, L., Davies, S.W., Penney, J.B., Bates, G.P. and Young, A.B. (1998) Altered brain neurotransmitter receptors in transgenic mice expressing a portion of an abnormal human Huntington disease gene. *Proc. Natl Acad. Sci. USA*, **95**, 6480–6485.
4. Cha, J.-H., Frey, A.S., Alsdorf, S.A., Kerner, J.A., Kosinski, C.M., Mangiarini, L., Penney, J.B., Davies, S.W., Bates, G.P. and Young, A.B. (1999) Altered neurotransmitter receptor expression in transgenic mouse models of Huntington's disease. *Phil. Trans. R. Soc. Lond. B Biol. Sci.*, **354**, 981–989.
5. Li, S.H., Cheng, A.L., Li, H. and Li, X.J. (1999) Cellular defects and altered gene expression in PC12 cells stably expressing mutant huntingtin. *J. Neurosci.*, **19**, 5159–5172.
6. Huang, C.C., Faber, P.W., Persichetti, F., Mittal, V., Vonsatte, J.-P., MacDonald, M.E. and Gusella, J.F. (1998) Amyloid formation by mutant huntingtin: threshold, progressivity and recruitment of normal polyglutamine proteins. *Somat. Cell Mol. Genet.*, **24**, 217–233.
7. Boutell, J.M., Thomas, P., Neal, J.W., Weston, V.J., Duce, J., Harper, P.S. and Jones, A.L. (1999) Aberrant interactions of transcriptional repressor proteins with the Huntington's disease gene product, huntingtin. *Hum. Mol. Genet.*, **8**, 1647–1655.
8. Lipshutz, R.J., Fodor, S.P., Gingeras, T.R. and Lockhart, D.J. (1999) High density synthetic oligonucleotide arrays. *Nature Genet.*, **21** (suppl. 1), 20–24.
9. Clagett-Dame, M. and Plum, L.A. (1997) Retinoid-regulated gene expression in neural development. *Crit. Rev. Eukaryot. Gene Expr.*, **7**, 299–342.
10. Matkovits, T. and Christakos, S. (1995) Ligand occupancy is not required for vitamin D receptor and retinoid receptor-mediated transcriptional activation. *Mol. Endocrinol.*, **9**, 232–242.
11. Horlein, A.J., Nar, A.M., Heinzel, T., Torchia, J., Gloss, B., Kurokawa, R., Ryan, A., Kamel, Y., Soderstrom, M., Glass, C.K. and Rosenfeld, M.G. (1995) Ligand-independent repression by the thyroid hormone receptor mediated by a nuclear receptor co-repressor. *Nature*, **377**, 397–404.
12. Toresson, H., Urquiza, A.M., Fagerstrom, C., Perlmann, T. and Campbell, K. (1999) Retinoids are produced by glia in the lateral ganglionic eminence and regulate striatal neuron differentiation. *Development*, **126**, 1317–1326.
13. Samad, T.A., Krezel, W., Chambon, P. and Borrelli, E. (1997) Regulation of dopaminergic pathways by retinoids: activation of the D2 receptor promoter by members of the retinoic acid receptor-retinoic X receptor family. *Proc. Natl Acad. Sci. USA*, **94**, 14349–14354.
14. Jonk, L.J.C., deJonge, M.E.J., Vervaart, J.M.A., Wissink, S. and Kruijer, W. (1994) Isolation and developmental expression of retinoic-acid-induced genes. *Dev. Biol.*, **161**, 604–614.
15. Bain, G., Ray, W.J., Yao, M. and Gottlieb, D.I. (1994) From embryonal carcinoma cells to neurons: the P19 pathway. *Bioessays*, **16**, 343–348.
16. Kogner, P., Borgstrom, P., Bjellerup, P., Schilling, F.H., Refai, E., Jonsson, C., Dominici, C., Wassberg, E., Bihl, H. and Jacobsson, H., Theodorsson, E. and Hassan, M. (1997) Somatostatin in neuroblastoma and ganglioneuroma. *Eur. J. Cancer*, **33**, 2084–2089.

17. Sato, T., Xiao, D.M., Li, H., Huang, F.L. and Huang, K.P. (1995) Structure and regulation of the gene encoding the neuron-specific protein kinase C substrate neurogranin (RC3 protein). *J. Biol. Chem.*, **270**, 10314–10322.
18. Pennypacker, K.R., Kincaid, R.L., Polli, J.W. and Billingsley, M.L. (1989) Expression of calmodulin-dependent phosphodiesterase, calmodulin-dependent protein phosphatase and other calmodulin-binding proteins in human SMS-KCNR neuroblastoma cells. *J. Neurochem.*, **52**, 1438–1448.
19. Lipskaia, L., Djiane, A., Defer, N. and Hanoune, J. (1997) Different expression of adenylyl cyclase isoforms after retinoic acid induction of P19 teratocarcinoma cells. *FEBS Lett.*, **415**, 275–280.
20. Kihira, H., Hiasa, A., Yamamoto, M., Katayama, N., Kuno, T, Ohtsuka, K., Shiku, H. and Nishikawa, M. (1998) Possible involvement of calcineurin in retinoic acid-induced inhibition of leukemic HL-60 cell proliferation. *Int. J. Oncol.*, **12**, 629–634.
21. Comb, M., Mermod, N., Hyman, S.E., Pearlberg, J., Ross, M.E. and Goodman, H.M. (1988) Proteins bound at adjacent DNA elements act synergistically to regulate human proenkephalin cAMP inducible transcription. *EMBO J.*, **7**, 3798–3805.
22. Montminy, M.R., Low, M.J., Tapia-Arancibia, L., Reichlin, S., Mandel, G. and Goodman, R.H. (1986) Cyclic AMP regulates somatostatin mRNA accumulation in primary diencephalic cultures and in transfected fibroblasts. *J. Neurosci.*, **6**, 1171–1176.
23. Laprade, N. and Soghomonian, J.J. (1997) Glutamate decarboxylase (GAD65) gene expression is increased by dopamine receptor agonists in a subpopulation of rat striatal neurons. *Brain Res. Mol. Brain Res.*, **48**, 333–345.
24. Reutter, M.A., Richards, E.M. and Sumners, C. (1997) Regulation of alpha 2A-adrenergic receptor mRNA in rat astroglial cultures: role of cyclic AMP and protein kinase C. *J. Neurochem.*, **68**, 47–57.
25. Du, Y., Carlock, L. and Kuo, T.H. (1995) The mouse plasma membrane Ca^{2+} pump isoform 1 promoter: cloning and characterization. *Arch. Biochem. Biophys.*, **316**, 302–310.
26. Matranga, V., Oliva, D., Sciarrino, S., D'Amelio, L. and Giallongo, A. (1993) Differential expression of neuron-specific enolase mRNA in mouse neuroblastoma cells in response to differentiation inducing agents. *Cell. Mol. Neurobiol.*, **13**, 137–145.
27. Vaccarino, F.M., Hayward, M.D., Le, H.N., Hartigan, D.J., Duman, R.S. and Nestler, E.J. (1993) Induction of immediate early genes by cyclic AMP in primary cultures of neurons from rat cerebral cortex. *Brain Res. Mol. Brain Res.*, **19**, 76–82.
28. Kuzhikandathil, E.V. and Molloy, G.R. (1994) Transcription of the brain creatine kinase gene in glial cells is modulated by cyclic AMP-dependent protein. *J. Neurosci. Res.*, **39**, 70–82
29. Rubinsztein, D.C., Leggo, J., Chiano, M., Dodge, A., Norbury, G., Rosser, E. and Craudfurd, D. (1997) Genotypes at the GluR6 kainate receptor locus are associated with variation in the age of onset of Huntington's disease. *Proc. Natl Acad. Sci. USA*, **94**, 3872–3876.
30. Schousboe, A., Belhage, B. and Frandsen, A. (1997) Role of Ca^{2+} and other second messengers in excitatory amino acid receptor mediated neurodegeneration: clinical perspectives. *Clin. Neurosci.*, **4**, 194–198.
31. Hodgson, J.G., Agopyan, N., Gutekunst, C.A., Leavitt, B.R., LePiane, F., Singaraja, R., Smith, D.J., Bissada, N., McCutcheon, K., Nasir, J. *et al.* (1999) A YAC mouse model for Huntington's disease with full-length mutant huntingtin, cytoplasmic toxicity and selective striatal neurodegeneration. *Neuron*, **23**, 181–192.
32. Bao, J., Sharp, A.H., Wagster, M.V., Becher, M., Schilling, G., Ross, C.A., Dawson, V.L. and Dawson, T.M. (1996) Expansion of polyglutamine repeat in huntingtin leads to abnormal protein interactions involving calmodulin. *Proc. Natl Acad. Sci. USA*, **93**, 5037–5042.
33. Mangiarini, L., Sathasivam, K., Seller, M., Cozens, B., Harper, A., Hetherington, C., Lawton, M., Trottier, Y., Lehrach, H., Davies, S.W. and Bates, G.P. (1996) Exon 1 of the HD gene with an expanded CAG repeat is sufficient to cause a progressive neurological phenotype in transgenic mice. *Cell*, **87**, 493–506.
34. Hurlbert, M.S., Zhou, W., Wasmeier, C., Kaddis, F.G., Hutton, J.C. and Freed, C.R. (1999) Mice transgenic for an expanded CAG repeat in the Huntington's disease gene develop diabetes. *Diabetes*, **48**, 649–651.
35. Dandoy-Dron, F., Guillo, F., Benboudjema, L., Deslys, J.P., Lasmezas, C., Dormont, D., Tovey, M.G. and Dron, M. (1998) Gene expression in scrapie. Cloning of a new scrapie-responsive gene and the identification of increased levels of seven other mRNA transcripts. *J. Biol. Sci.*, **273**, 7691–7697.
36. Greengard, P., Allen, P.B. and Nairn, A.C. (1999) Beyond the dopamine receptor: the DARPP-32/protein phosphatase-1 cascade. *Neuron*, **23**, 435–447.
37. Schilling, G., Becher, M.W., Sharp, A.H., Jinnah, H.A., Duan, K., Kotzuk, J.A., Slunt, H.H., Ratovitski, T., Cooper, J.K., Jenkins, N.A., Copeland, N.G., Price, D.L., Ross, C.A. and Borchelt, D.R. (1999) Intranuclear inclusions and neuritic aggregates in transgenic mice expressing a mutant N-terminal fragment of huntingtin. *Hum. Mol. Genet.*, **8**, 397–407.
38. Menalled, L., Zanjani, H., MacKenzie, L., Koppel, A., Carpenter, E., Zeitlin, S. and Chesselet, M.-F. (2000) Decrease in striatal enkephalin mRNA in mouse models of Huntington's disease. *Exp. Neurol.*, **162**, 328–342.
39. Albin, R.L., Qin, Y., Young, A.B., Penney, J.B. and Chesselet, M.F. (1991) Preproenkephalin messenger RNA-containing neurons in striatum of patients with symptomatic and presymptomatic Huntington's disease: an *in situ* hybridization study. *Ann. Neurol.*, **30**, 542–549.
40. Augood, S.J., Faull, R.L.M., Love, D.R. and Emson, P.C. (1996) Reduction in enkephalin and substance P messenger RNA in the striatum of early grade Huntington's disease: a detailed cellular *in situ* hybridization study. *Neuroscience*, **72**, 1023–1036.
41. Marangos, P.J. and Paul, S.M. (1981) Brain levels of neuron-specific and nonneuronal enolase in Huntington's disease. *J. Neurochem.*, **37**, 1338–1340.
42. Tanaka, C., Nishino, N., Hashimoto, T., Kitamura, N., Yoshihara, C. and Saito, N. (1993) Second messenger systems in brains of patients with Parkinson's or Huntington's disease. *Adv. Neurol.*, **60**, 175–180.
43. Enna, S.J., Bird, E.D., Bennett, J.P., Bylund, D.B., Yammura, H.I., Iversen, L.L. and Snyder, S.H. (1976) Huntington's chorea: changes in neurotransmitter receptors in the brain. *N. Engl. J. Med.*, **294**, 1305–1309.
44. Warsh, J.J., Politsky, J.M., Li, P.P., Kish, S.J. and Hornykiewicz, O. (1991) Reduced striatal [^{3}H]inositol 1, 4, 5-trisphosphate binding in Huntington's disease. *J. Neurochem.*, **56**, 1417–1422.
45. Sen, A.P., Boksa, P. and Quirion, R. (1993) Brain calcium channel related dihydropyridine and phenylalkylamine binding sites in Alzheimer's, Parkinson's and Huntington's diseases. *Brain Res.*, **611**, 216–221.
46. Glass, M., Faull, R.L.M. and Dragunow, M. (1993) Loss of cannabinoid receptors in the substantia nigra in Huntington's disease. *Neuroscience*, **56**, 523–527.
47. Robertson, H.A., MacDonald, C.J. and Denovan-Wright, E.M. (1999) Cannabinoid receptor (CB1) mRNA loss in the lateral striatum of Huntington's disease transgenic mice. *Soc. Neurosci. Abstr.*, **25** (Part 1), 829.
48. Tallman, M.S. (1998) Therapy of acute promyelocytic leukemia: all-trans retinoic acid and beyond. *Leukemia*, **12** (suppl. 1), S37–S40.
49. Carter, R.J., Lione, L.A., Humby, T., Mangiarini, L., Mahal, A., Bates, G.P., Dunnett, S.B. and Morton, A.J. (1999) Characterization of progressive motor deficits in mice transgenic for the human Huntington's disease mutation. *J. Neurosci.*, **19**, 3248–3257.
50. Ross, C.A., Wood, J.D., Schilling, G., Peters, M.F., Nucifora Jr, F.C., Cooper, J.K., Sharp, A.H., Margolis, R.L. and Borchelt, D.R. (1999) Polyglutamine pathogenesis. *Phil. Trans. R. Soc. Lond. B Biol. Sci.*, **354**, 1005–1011.
51. Cooper, J.K., Schilling, G., Peters, M.F., Herring, W.J., Sharp, A.H., Kaminsky, Z., Masone, J., Khan, F.A., Delanoy, M., Borchelt, D.R. *et al.* (1998) Truncated N-terminal fragments of huntingtin with expanded glutamine repeats form nuclear and cytoplasmic aggregates in cell culture. *Hum. Mol. Genet.*, **7**, 783–790.
52. DiFiglia, M., Sapp, E., Chase, K.O., Davies, S.W., Bates, G.P., Vonsattel, J.-P. and Aronin, N. (1997) Aggregation of huntingtin in neuronal intranuclear inclusions and dystrophic neurites in brain. *Science*, **277**, 1990–1993.
53. Sittler, A., Walter, S., Wedemeyer, N., Hasenbank, R., Scherzinger, E., Eickhoff, H., Bates, G.P., Lehrach, H. and Wanker, E.E. (1998) SH3GL3 associates with the Huntingtin exon 1 protein and promotes the formation of polygln-containing protein aggregates. *Mol. Cell*, **2**, 427–436.
54. Faber, P.W., Barnes, G.T., Srinidhi, J., Chen, J., Gusella, J.F. and MacDonald, M.E. (1998) Huntingtin interacts with a family of WW domain proteins. *Hum. Mol. Genet.*, **7**, 1463–1474.
55. Landwehrmeyer, G.B., McNeil, S.M., Dure, L.S., Ge, P., Aizawa, H., Huang, Q., Ambrose, C.M., Duyao, M.P., Bird, E.D., Bonilla, E. *et al.* (1995) Huntington's disease gene: regional and cellular expression in brain of normal and affected individuals. *Ann. Neurol.*, **37**, 218–230.
56. Augood, S.J., Faull, R.L.M. and Emson, P.C. (1997) Dopamine D1 and D2 receptor gene expression in the striatum in Huntington's disease. *Ann. Neurol.*, **42**, 215–221.

57. Richfield, E.K., Young, A.B. and Penney, J.B. (1986) Properties of D2 dopamine receptor autoradiography: high percentage of high-affinity agonist sites and increased nucleotide sensitivity in tissue sections. *Brain Res.*, **383**, 121–128.
58. Cox, R.F. and Waszczak, B.L. (1991) Autoradiography of dopamine D2 receptors using [^{3}H]YM-09151-2. *Eur. J. Pharmacol.*, **199**, 103–106.
59. Jarvis, M.F. and Williams, M. (1989) Direct autoradiographic localization of adenosine A2 receptors in the rat brain using the A2-selective agonist, [^{3}H]CGS 21680. *Eur. J. Pharmacol.*, **168**, 243–246.
60. Worley, P.F., Baraban, J.M., De Souza, E.B. and Snyder, S.H. (1986) Mapping second messenger systems in the brain: differential localizations of adenylate cyclase and protein kinase C. *Proc. Natl Acad. Sci. USA*, **83**, 4053–4057.